

## Nearest-Neighbor-Atom Core-Hole Transfer in Isolated Molecules

R. Guillemin,<sup>1</sup> O. Hemmers,<sup>1</sup> D. Rolles,<sup>2,3</sup> S.W. Yu,<sup>1,2</sup> A. Wolska,<sup>1</sup> I. Tran,<sup>1</sup> A. Hudson,<sup>1</sup> J. Baker,<sup>1</sup> and D.W. Lindle<sup>1</sup>

<sup>1</sup>*Department of Chemistry, University of Nevada, Las Vegas, Nevada 89154-4003, USA*

<sup>2</sup>*Advanced Light Source, Lawrence Berkeley National Laboratory, Berkeley, California 94720, USA*

<sup>3</sup>*Fritz-Haber-Institut der Max-Planck Gesellschaft, Berlin, Germany*

(Received 3 February 2004; published 3 June 2004)

A new phenomenon sensitive only to next-door-neighbor atoms in isolated molecules is demonstrated using angle-resolved photoemission of site-selective core electrons. Evidence for this interatomic core-to-core electron interaction is observable only by measuring nondipolar angular distributions of photoelectrons. In essence, the phenomenon acts as a very fine atomic-scale sensor of nearest-neighbor elemental identity.

DOI: 10.1103/PhysRevLett.92.223002

PACS numbers: 33.60.Fy, 33.80.Eh

For decades, photoelectron spectroscopy (PES) has been an established method for probing the electronic and chemical structure of matter in both gaseous and condensed phases [1]. Coupled with a tunable light source, such as synchrotron radiation, PES is often done resonantly; e.g., direct photoemission intensity from an outer (valence) orbital or energy level is modified in a narrow wavelength range by interference with resonant excitation of an electron in a deeper-lying (core) orbital. Recently, a new phenomenon, multiatom resonant photoemission (MARPE), was reported in condensed phase MnO [2–4] in which the *core-level* photoemission intensity, or cross section, from one element (O) is enhanced upon resonant excitation of a *core electron* from a different element (Mn) in the solid. The unprecedented core-to-core interaction represented by MARPE is explained as a collective resonant effect from several nearby atoms and has been proposed as a new tool for identifying near-neighbor atoms (within 2 nm) in solids. Reports of MARPE have engendered both interest and skepticism in the photoemission community [5,6]. From an isolated-molecule point of view, MARPE is an unusual form of resonant-Auger decay and can be understood as an interatomic coupling between direct core-electron photoemission from one atom and resonant core-electron excitation of a different atom in the same molecule. Up to now, attempts to find experimental evidence for this MARPE-like effect in small gas-phase molecules by looking for variations in photoemission intensities, whether integrated (cross sections) or differential (angular-distribution parameters), have been in vain.

In this Letter we report the first evidence of an interatomic coupling effect in molecular photoemission solely involving core levels. To distinguish it from the relatively longer-range MARPE effect, the inherently short-range (i.e., nearest-neighbor-only) effect in isolated molecules will be referred to as nearest-neighbor-atom core-hole transfer, or NACHT. While solid-state MARPE affects photoemission cross sections, no such intensity variations

are observable in the molecular analog; the NACHT effect is measurable *only* in the differential cross section, which describes the angular distributions of photoelectrons and is sensitive to the phases of the photoelectrons' continuum wave functions, as well as their magnitudes. Moreover, it is necessary to consider differential-cross-section effects beyond the usual dipole approximation (DA) for interactions between radiation and matter. The electric DA is essentially a uniform-electric-field approximation assuming negligible spatial variation of the electric field of the ionizing radiation over the dimensions of the absorbing charge distribution (i.e., the molecular orbital); thus, the expansion of  $\exp(i\mathbf{k}_p \cdot \mathbf{r})$  describing the quantum-mechanical interaction of a photon field and an electron is reduced to its simplest possible form, unity. In the DA, all higher-order effects, such as electric-quadrupole and magnetic-dipole interactions, are neglected.

Although well-known breakdowns of the DA exist for photon energies higher than  $\sim 10$  keV (wavelengths below  $\sim 1$  Å), quantitatively significant breakdowns at much lower energies, below 1 keV, were demonstrated in unexpected ways for atoms and molecules only fairly recently [7,8]. Going beyond the zeroth-order DA, but only to first order in the photon momentum by truncating the expansion of  $\exp(i\mathbf{k}_p \cdot \mathbf{r})$  at  $1 + \mathbf{k}_p \cdot \mathbf{r}$ , the parametrization of Cooper [9,10] yields the following expression for the differential photoionization cross section describing the angular distribution of photoelectrons ionized from a randomly oriented target by 100% linearly polarized light:

$$\frac{d\sigma(h\nu)}{d\Omega} = \frac{\sigma(h\nu)}{4\pi} \{ [1 + \beta(h\nu)P_2(\cos\theta_e)] + [\delta(h\nu) + \gamma(h\nu)\cos 2\theta_e] \sin\theta_e \cos\phi_e \}. \quad (1)$$

On the right-hand side of Eq. (1), the first two terms constitute precisely the well-known expression for the differential cross section in the DA [11], with  $\theta_e$  the polar angle of electron emission relative to the photon

polarization,  $\sigma(h\nu)$  the photoionization cross section, and  $\beta(h\nu)$  the (dipolar) angular-distribution parameter. The full Eq. (1) represents the first-order-nondipolar differential cross section, where  $\phi_e$  is the azimuthal angle of electron emission relative to the photon-beam direction, and  $\delta(h\nu)$  and  $\gamma(h\nu)$  are the (first-order-)nondipolar angular-distribution parameters. These new nondipole parameters result from  $E_1 \otimes (E_2, M_1)$  interference terms between electric-dipole  $E_1$  and electric-quadrupole  $E_2$  or magnetic-dipole  $M_1$  terms in the description of the photon interaction [10], although the  $M_1$  contributions are expected to be negligible at photon energies below 1 keV. The  $\cos\phi_e$  term introduces a potential forward/backward asymmetry, relative to the photon propagation vector, into the photoelectron emission intensity. Note this first-order-nondipole correction does not affect the photoionization cross section but only the angular distributions of the photoelectrons; i.e., nondipole photoemission, as discussed herein, is reflected only in a spatial redistribution of electron emission. Recent molecular-photoemission measurements at photon energies not far above the  $N_2$   $K$  edge, accompanied by a detailed theoretical analysis [8], have already demonstrated first-order-nondipole effects can be a sensitive probe of photoemission dynamics, as well as molecular structure through bond-length-dependent  $E_1 \otimes (E_2, M_1)$  terms [12].

In the present work, we investigate nondipolar angular distributions of core-level photoelectrons from two simple linear triatomic molecules, nitrous oxide and carbonyl sulphide. The ground-state  $N_2O$  molecule has the geometry  $N_t-N_c-O$ , where  $N_t$  and  $N_c$  label terminal and central-nitrogen atoms, respectively. The two nitrogens are inequivalent owing to their different chemical environments, leading to chemical shifts affecting the ionization energies (thresholds) of the N 1s core levels; the binding energies of the  $N_t$  and  $N_c$  1s core electrons are 408.5 and 412.5 eV, respectively [13]. The 4-eV relative chemical shift allows PES measurements to easily identify the atomic site of the molecule being ionized. About 130 eV above the nitrogen thresholds lies the O 1s ionization threshold at 541.4 eV. To search for NACHT effects, direct photoemission from the two inequivalent N 1s core levels was probed in the vicinity of the resonant excitation, at 534.6 eV, of an O 1s electron to the lowest unoccupied  $3\pi^*$  molecular orbital [14]. Figure 1 shows photoabsorptionlike spectra measured using total electron yield as a function of photon energy in the vicinity of the  $N_t$ ,  $N_c$ , and O 1s thresholds.

The PES experiment was performed at beam line 8.0.1.3 of the Advanced Light Source (ALS). The undulator radiation passed through a monochromator that permitted selecting or continuously scanning the photon energy with a resolving power up to 8000 in the region of interest. The monochromatic radiation is also 100% linearly polarized. The experimental setup has been described in detail elsewhere [15]. Briefly, three time-of-

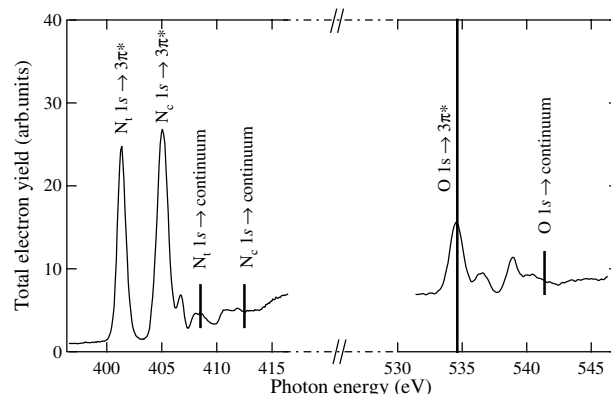


FIG. 1. Total-electron-yield spectra in the vicinity of the  $N_t$ ,  $N_c$ , and O  $K$  edges of  $N_2O$  as a function of photon energy. Intensities in the spectra are not directly comparable.

flight electron spectrometers were used to collect photoelectron spectra simultaneously at three selected angles. Angular-distribution parameters are determined by comparing normalized peak intensities among the three analyzers. For measurements in the nominal experimental geometry, for which  $\delta$  and  $\gamma$  are unresolvable, it is convenient to introduce the combined nondipole parameter  $\zeta = 3\delta + \gamma$ . For  $N_2O$ , intensities of the  $N_t$  and  $N_c$  1s photoelectron peaks were determined via a fitting procedure allowing accurate separation of the two contributions to the spectra. Normalization of peak intensities in different analyzers was achieved via a calibration procedure, as a function of electron kinetic energy, using argon 2p photoemission, for which the dipolar and nondipolar angular-distribution parameters are known accurately from theory and experiment [16].

Although values of  $\beta$  and  $\zeta$  for all three core shells in  $N_2O$  were measured over a wide photon-energy range, this work focuses on the results for  $N_c$  and  $N_t$  1s photoelectrons near the O 1s  $\rightarrow 3\pi^*$  resonance, about 7 eV below the O 1s threshold. The  $N_t/N_c$  cross-section ratio measured in this energy region is shown in Fig. 2(a), and the corresponding results for  $\beta$  for both levels are included in Fig. 2(b). The ratio is constant within the experimental uncertainties of  $\pm 5\%$ , showing no signs of coupling to the O 1s  $\rightarrow 3\pi^*$  resonance, although a slight systematic variation may be present. A similar result is observed for both dipolar angular-distribution parameters. To zeroth order, then,  $N_2O$  photoemission exhibits no evidence of a (dipolar) NACHT effect (D-NACHT). In contrast, the measured nondipole  $\zeta$  parameters for  $N_t$  and  $N_c$  1s photoelectrons, shown in Figs. 2(c) and 2(d), respectively, exhibit evidence of an interatomic coupling effect, particularly in the case of the central-nitrogen atom, the one *closest* to the originally excited oxygen atom. Thus, the significant effect in Fig. 2(d) marks the first observation of the MARPE-like NACHT effect in an isolated molecule. Because it appears only in the nondipole parameter  $\zeta$ , it is clear the core-to-core interaction

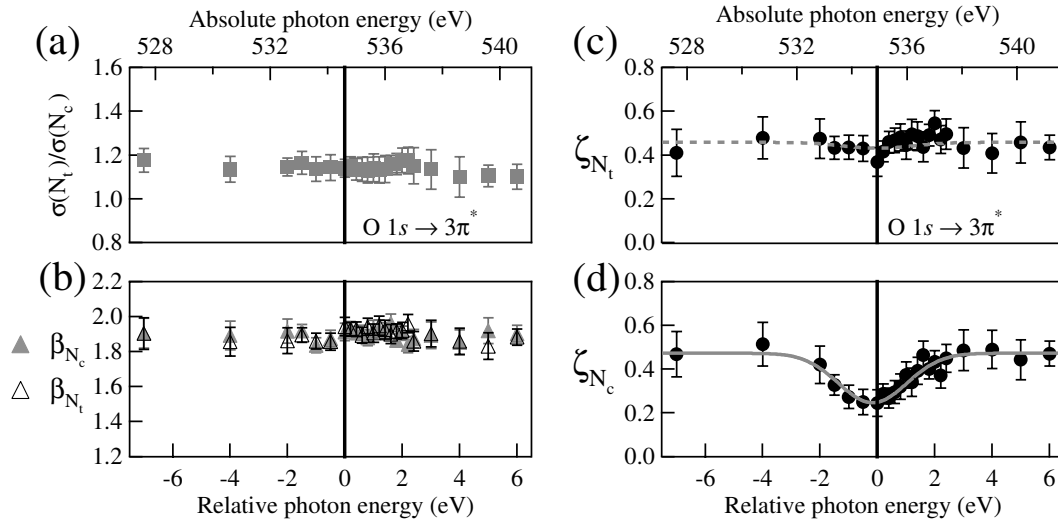


FIG. 2. (a) Partial-cross-section ratio  $\sigma(N_t)/\sigma(N_c)$  for N  $1s$  photoemission from  $N_2O$  in the vicinity of the O  $1s \rightarrow 3\pi^*$  resonance (vertical line). (b) Dipole parameters  $\beta$  for  $N_t$  and  $N_c$   $1s$  photoelectrons. (c) Nondipole parameter  $\zeta = 3\delta + \gamma$  for  $N_t$   $1s$  photoelectrons and for (d)  $N_c$   $1s$  photoelectrons. Error bars reflect statistical uncertainties only. The solid curve is a fit to the data, and the dashed curve is an estimate based on the solid curve (see text).

between the oxygen and central-nitrogen atoms is mediated by the quadrupole interaction with the ionizing radiation (again  $M_1$ -related terms are expected to be negligible), hence this phenomenon will be referred to as Q-NACHT. A quadrupole-mediated effect, as opposed to a dipole one (D-NACHT), is not surprising considering the quadrupole interaction emphasizes the higher- $r$  portion of electronic wave functions compared to the dipole interaction. In order to evaluate the influence of the bond length on the interatomic interaction, we used a simple model and the known bond lengths: O- $N_c = 1.186$  Å and  $N_t$ - $N_c = 1.127$  Å [17]. Unlike the  $3\pi^*$  molecular orbital which is an antibonding delocalized orbital (spreading over the dimension of the molecule), core  $1s$  orbitals are atomiclike and strongly localized around the atoms. By first fitting the profile of the  $\zeta$  curve in Fig. 2(d) (solid curve), we then estimated the amplitude of the Q-NACHT effect expected on the terminal nitrogen atom by assuming an exponential decay of the spatial extent of  $1s$  atomic core orbitals and calculating overlaps between the O,  $N_c$ , and  $N_t$   $1s$  orbitals. This very simple model indicates the distance between the oxygen and the terminal nitrogen is enough to reduce the amplitude of the effect on  $N_t$  to below our experimental error bars [dashed curve in Fig. 2(c)]. It is interesting to note both  $N_t$  and  $N_c$   $1s$  photoemission show distinct forward-directed asymmetries at photon energies away from the O  $1s \rightarrow 3\pi^*$  resonance. Curiously, coupling of  $N_c$   $1s$  photoemission with the O  $1s$  resonance removes some of the nondipolar azimuthal anisotropy in the angular distribution.

To confirm the  $N_2O$  results, a similar measurement was performed on linear O-C-S; it exhibits the same nearest-neighbor Q-NACHT effect. Ionization energies

for OCS are 540.3 eV for O  $1s$  [18], 295.5 eV for C  $1s$  [19], and 170.3 and 171.6 eV for S  $2p_{3/2}$  and  $2p_{1/2}$ , respectively [19]. About 7.2 eV below the O  $1s$  threshold lies the O  $1s \rightarrow 4\pi^*$  resonance at 533.1 eV [18]. Similarly, the  $4\pi^*$  resonance is about 7.3 eV below the C  $1s$  threshold at 288.23 eV [19]. Figure 3 summarizes  $\zeta$  measurements for C  $1s$  and S  $2p$  photoelectrons in the vicinity of the O  $1s \rightarrow 4\pi^*$  resonance [Fig. 3(a)] and for S  $2p$  photoelectrons near the C  $1s \rightarrow 4\pi^*$  resonance [Fig. 3(b)].

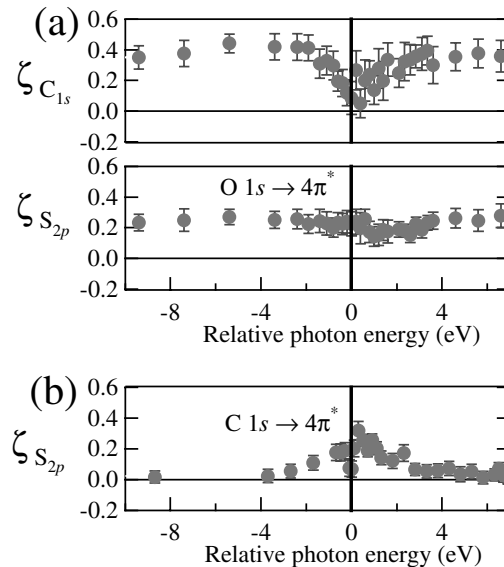


FIG. 3. (a) Nondipole parameter  $\zeta$  for C  $1s$  and S  $2p$  photoelectrons in the vicinity of the O  $1s \rightarrow 4\pi^*$  resonance (vertical line) in OCS. (b) Nondipole parameter  $\zeta$  for S  $2p$  photoelectrons in the vicinity of the C  $1s \rightarrow 4\pi^*$  resonance (vertical line).

As with  $\text{N}_2\text{O}$ , no effects were observed in either the relative cross sections or the  $\beta$  parameters (not shown) within experimental error. The results in Fig. 3 confirm the nearest-neighbor sensitivity of Q-NACHT as demonstrated in  $\text{N}_2\text{O}$ ; the nondipolar angular distribution of C  $1s$  photoelectrons is perturbed by the O  $1s \rightarrow 4\pi^*$  resonance but, within experimental uncertainty, no influence is observed on S  $2p$  photoemission at this resonance. However, a Q-NACHT effect is observed for S  $2p$  photoemission when scanning through the C  $1s \rightarrow 4\pi^*$  resonance excited from the neighboring carbon atom. Somewhat surprisingly, the two Q-NACHT effects observed in Fig. 3 lead to opposite changes in forward/backward asymmetries. While only a complete theoretical analysis can properly explain this difference, it is likely the relative phases of the S  $2p$  and C  $1s$  photoelectron continuum wave functions at the initially excited atomic sites (C and O, respectively) influence this behavior. In any case, the combined results from  $\text{N}_2\text{O}$  and OCS clearly demonstrate Q-NACHT effects depend on core-to-core coupling only between immediate neighbors.

To conclude, it is of interest to compare NACHT to other spectroscopic methods. While MARPE is observed to first decrease and then increase the intensity of photoelectron emission upon crossing a resonance, following a form reminiscent of a Fano profile [4], NACHT, so far, is expressed only in nondipolar angular distributions. MARPE is a multiatom effect, involving a collective contribution of neighboring atoms within a range of about 2 nm, whereas the NACHT effect seems to involve just two atoms, the emitter and its nearest neighbor, and is naturally limited to a much smaller interaction distance. Extended x-ray absorption fine structure, in which oscillations in the x-ray-absorption coefficient are related to bond lengths in the sample (usually a solid), also probes atoms nearby to the initially ionized atom. Unlike NACHT, it is not directly sensitive to the identity of the neighboring species. Finally, the NACHT phenomenon can be likened to the x-ray equivalent of a pump-probe experiment with a single photon. In this analogy, the incident x radiation can be thought of as pumping a well-defined atomic site in a molecule (e.g., O in  $\text{N}_2\text{O}$ ). But, because photoionization is a quantum phenomenon, the incident radiation also can interact with the N  $1s$  electrons on the neighboring  $\text{N}_c$  atoms. This duality essentially allows the latter interaction (with the  $\text{N}_c$  in  $\text{N}_2\text{O}$ ) to act as the “probe” of the resonant interaction with the initial atomic site (O). Furthermore, because NACHT is mediated by the (weaker) quadrupole interaction, it is sensitive over a very short distance, yielding a unique probe of only nearest-neighbor atoms.

This work was supported by NSF Grant No. PHY-01-40375. The ALS (LBNL) was supported by DOE,

Materials Science Division, BES, OER under Contract No. DE-AC03-76SF00098.

- 
- [1] *VUV and Soft X-Ray Photoionization*, edited by U. Becker and D. A. Shirley (Plenum Press, New York, 1996); J. Berkowitz, *Photoabsorption, Photoionization, and Photoelectron Spectroscopy* (Academic Press, New York, 1979); *X-Ray and Inner-Shell Processes*, edited by T. A. Carlson, M. O. Krause, and S. T. Manson (American Institute of Physics, New York, 1990).
  - [2] A. Kay, E. Arenholz, S. Mun, F. J. García de Abajo, C. S. Fadley, R. Denecke, Z. Hussain, and M. A. Van Hove, *Science* **281**, 679 (1998).
  - [3] F. J. García de Abajo, C. S. Fadley, and M. A. Van Hove, *Phys. Rev. Lett.* **82**, 4126 (1999).
  - [4] A. W. Kay, F. J. Garcia de Abajo, S.-H. Yang, E. Arenholz, B. S. Mun, N. Mannellea, Z. Hussain, M. A. Van Hove, and C. S. Fadley, *Phys. Rev. B* **63**, 115119 (2001).
  - [5] A. Moewes, E. Z. Kurmaev, D. L. Ederer, and T. A. Callcott, *Phys. Rev. B* **62**, 15427 (2000).
  - [6] D. Nordlund, M. G. Garnier, N. Witkowski, R. Denecke, A. Nilsson, M. Nagasono, N. Mårtensson, and A. Fölsch, *Phys. Rev. B* **63**, 121402 (2001).
  - [7] D. W. Lindle and O. Hemmers, *J. Electron Spectrosc. Relat. Phenom.* **100**, 297 (1999).
  - [8] O. Hemmers, H. Wang, P. Focke, I. A. Sellin, D. W. Lindle, J. C. Arce, J. A. Sheehy, and P. W. Langhoff, *Phys. Rev. Lett.* **87**, 273003 (2001).
  - [9] J. W. Cooper, *Phys. Rev. A* **42**, 6942 (1990).
  - [10] J. W. Cooper, *Phys. Rev. A* **47**, 1841 (1993).
  - [11] J. Cooper and R. N. Zare, *J. Chem. Phys.* **48**, 942 (1968).
  - [12] P. Langhoff, J. C. Arce, J. A. Sheehy, O. Hemmers, H. Wang, P. Focke, I. A. Sellin, and D. W. Lindle, *J. Electron Spectrosc. Relat. Phenom.* **114**, 23 (2001).
  - [13] M. Schmidbauer, A. L. D. Kilcoyne, K. J. Randall, J. Feldhaus, A. M. Bradshaw, M. Braunstein, and V. McCoy, *J. Chem. Phys.* **94**, 5299 (1991).
  - [14] J. I. Adachi and N. Kosugi, *J. Chem. Phys.* **102**, 7369 (1995).
  - [15] O. Hemmers, S. B. Whifield, P. Glans, H. Wang, D. W. Lindle, R. Wehlitz, and I. A. Sellin, *Rev. Sci. Instrum.* **69**, 3809 (1998).
  - [16] For theory, see A. Derevianko, W. R. Johnson, and K. T. Cheng, *At. Data Nucl. Data Tables* **73**, 153 (1999). Experimental results are unpublished but are in excellent agreement with theory.
  - [17] F. A. Grimm, T. A. Carlson, J. Jiménez-Mier, B. Yates, J. W. Taylor, and B. P. Pullen, *J. Electron Spectrosc. Relat. Phenom.* **47**, 257 (1988).
  - [18] T. K. Sham, B. X. Yang, J. Kirz, and J. S. Tse, *Phys. Rev. A* **40**, 652 (1989).
  - [19] P. Erman, A. Karawajczyk, E. Rachlew, M. Stankiewicz, and K. Yoshiki Franzén, *Phys. Rev. A* **56**, 2705 (1997).